CGU HS Committee on River Ice Processes and the Environment
17th Workshop on River Ice
Edmonton, Alberta, July 21 - 24, 2013

Ice Thickness Prediction: A Comparison of Various Practical Approaches

George Comfort[1], and Razek Abdelnour[2]
[1]*G. Comfort Ice Engineering Ltd., 2 Conacher Gate, Kanata, Ont. K2K 3H1*
Comfortga@gmail.com

[2]*Geniglace Inc., 30 Berlioz, Suite 902, Verdun, Quebec H3e 3L3*
RazekAbdelnour@gmail.com

Abstract: The ice thickness is a fundamental parameter for practically all ice problems. Usually, the engineer is confronted with the problem of predicting the ice thickness, and often its return period as well, with little information. Many approaches are available, and they each have advantages and limitations. Ice thickness prediction methods vary from statistical analyses based on ice thickness data to a wide range of numerical ice thickness predictors.

At the simplest level, one can use empirical analyses based on the Freezing Degree Days (FDDS). This can be refined in various ways, especially if ice thickness data are available for calibration. Also, the authors have found that because the empirical coefficient for these predictors varies, improved accuracy can be obtained by incorporating this variability either in a statistical manner or in a deterministic manner based on its relationship with say, the ice thickness. Furthermore, the authors have found that a 2-stage approach is often useful where the results of purely statistical predictions based on ice thickness data are compared with probabilistic analyses combining the variability in both the FDDs and the empirical coefficient.

The authors have also used more complex methods based on heat transfer calculations that included snowfalls and rainfalls, and the buildup of slush on the ice thickness. This approach predicted the ice thickness, the snow depth, the slush on the ice surface and whether or not it refroze, and the ice temperature profile for each day of the winter. Of course, this approach requires more input data and computation effort. In this case, the method was developed based on more than 10 years of field data.

The most appropriate approach for predicting ice thicknesses depends on many factors including the application and the accuracy requirements; as well as the amount and quality of the available ice thickness data and, depending on the method used, the available supplementary environmental data.

The paper makes comparisons among various methods illustrated with a practical example from their experience. The paper concludes with overall comments and recommendations.

1. Introduction

The ice thickness is a fundamental parameter for practically all ice problems. Usually, the engineer is confronted with the problem of predicting the ice thickness, and often its return period as well, with little information. Many approaches are available, and they each have advantages and limitations. Ice thickness prediction methods vary from statistical analyses based on ice thickness data to a wide range of numerical ice thickness predictors. This paper compares methods for predicting static ice formation, in which the flow velocity plays no role. The threshold current for static ice formation is about 0.3m/s (USACE, 2002).

2. The Ice Growth Process and How it Affects Predictions of Ice Thickness

It is well-known that the ice growth process is complex, and that it varies from case to case. It is rare that the ice growth in a winter occurs entirely by thermal growth, but even when it does, the ice crystallography varies significantly with depth in the sheet. The buildup of a snow cover substantially retards the ice growth process. The occurrence of a snowfall also affects the ice growth process as it adds insulation to the ice surface causing the ice to warm from the "bottom up". During a 10-year field measurement program of static ice loads on dams, Comfort et al 2003a; 2003b found that snowfalls were a major contributor to about 70% of the thermal events.

Based on a purely thermal analysis, one would expect that the ice would grow entirely from the bottom downwards. However, field experience shows that this is often not the case. Several investigators have found that ice may be formed on the surface (termed ice surface growth here) due to various mechanisms, and they have observed that the ice profile is layered (Figure 1.1).

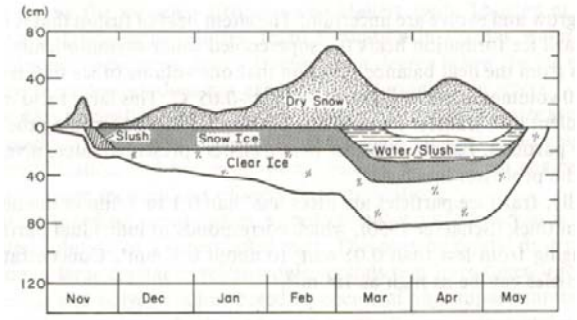

Figure 4-16. Ice growth on Lake Gäutajure, Sweden, during the winter of 1962–63. A large snowfall on 6-cm-thick ice in November resulted in 17 cm of slush, which subsequently refroze. A similar event occurred in March. (After Fremling 1977.)

Cited by Ashton, 1986

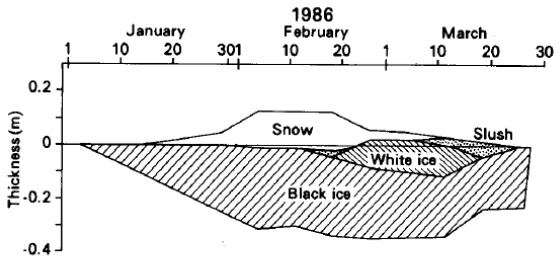

FIG. 2. Growth of ice in Lake Ontario at Kingston during 1986. Data are mean values from nine stations shown in Figure 1c and are plotted in relation to the free water level.

After Gilbert and Glew, 1986

Figure 1.1 Ice Layering

Ice surface growth can result from the freezing of slush formed on the ice surface, as was observed many times in the field (e.g., Comfort et al 2003a; 2003b). This resulted from various mechanisms. Slush was formed by rainfalls which added water to the ice surface as well as melting the snow that was already there; and then, this water and slush subsequently froze.

For deep snow cover, the weight of the snow depressed the ice surface below water level, causing water to flood onto the ice surface through cracks in the ice surface. Water reached the ice surface through cracks in the ice sheet which also melted some of the snow that subsequently froze. Often, not all of the surface water froze, leaving layers of water above the initial ice surface. This led to a situation where layers of snow, ice, and water were present above the ice sheet that was originally present. When water layers were present on the surface, no further ice growth was possible until, or unless, the water and slush froze.

In summary, there are often many external influences which affect the ice profile. This complicates efforts to develop an ice thickness predictor. One must strive for a balance between simplicity, in order to make the predictor usable and to be able to define all of the required inputs; and complexity, in order for the predictor to accurately represent the processes that occur.

3. Simplified Thermal Analyses

The ice thickness, h, produced by static ice formation is most commonly predicted based on the accumulated Freezing Degree Days (FDDs), as given below. This equation (commonly termed the Stefan equation) is derived by solving the differential equation for the thermal growth rate, and by making various simplifying assumptions (e.g., USACE, 2002).

$$h = \alpha * \sqrt{FDD} \qquad [3.1]$$

where α is an empirical coefficient that varies from site to site depending on local conditions such as the snow cover, winds, and solar radiation. Table 3.1 lists common values for "α".

Table 3.1 Values for the Stefan Equation Coefficient (USACE, 2002)

Table 2-1
Typical Values of α (after Michel 1971)

Ice Cover Condition	*α **	*α †*
Windy lake w/no snow	2.7	0.80
Average lake with snow	1.7–2.4	0.50–0.70
Average river with snow	1.4–1.7	0.40–0.50
Sheltered small river	0.7–1.4	0.20–0.40

* AFDD calculated using degrees Celsius. The ice thickness is in centimeters.
† AFDD calculated using degrees Fahrenheit. The ice thickness is in inches.

4. Detailed Mechanics-Based Ice Growth Models

4.1 Overview

Various investigators have developed detailed mechanics-based ice growth models. Singh and Comfort, 1998 developed a 1-D mechanics-based model for ice growth at hydro-electric

reservoirs (as an aid to assessing static ice loads on dams), based on the physical processes seen over at many sites over more than 10 years of field observations (Comfort et al, 2003a; 2003b). Morse et al, 2009 developed a similar model to describe ice growth in a tidal estuary.

Singh and Comfort, 1998's model was used here for sample calculations and comparisons as the authors are more familiar with it. Furthermore, no site-specific constants were incorporated into their model, and they found that it gave reasonable correlation with measured values at reservoirs in Manitoba, Ontario and Quebec. Thus, it was considered reasonable to attempt to apply the model to ice growth estimations elsewhere, for the case considered in this paper.

Singh and Comfort, 1998's model was set up to predict the following parameters sequentially for the whole winter starting with freeze-up: (a) the ice thickness; (b) the snow cover thickness; (c) the formation and thickness of slush; and (d) the ice temperature profile.

4.1 Ice Thickness

Singh and Comfort, 1998 noted that the reservoir ice sheet could be divided generally into two main ice types: (a) "bottom growth", consisting of ice formed downwards from the ice bottom; and (b) "surface growth", consisting primarily of snow ice formed on the ice surface by refrozen slush. Of course, the growth of these two types of ice was not fully independent because they depended on air temperature, and the snow cover thickness as illustrated in Figure 4.1.

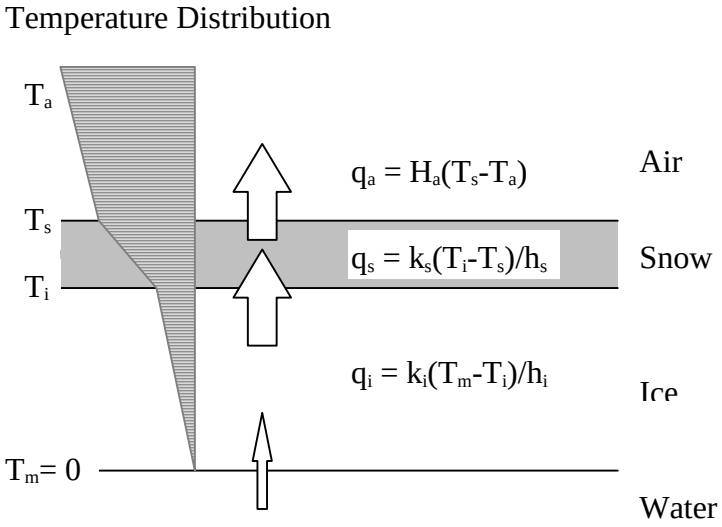

Figure 4.1 Heat Flux Through an Ice Cover

"Bottom Ice Growth"

This was estimated by balancing the heat flux from the ice surface to air with the heat flux required in the fusion of ice. It was assumed that the temperature was linearly distributed in the ice and the snow cover (as is commonly assumed, e.g., Ashton, 1986, and as was generally supported by field data – Comfort et al, 2003a; 2003b). The temperature varies from T_s at the

snow surface to T_i at the ice surface to 0°C at the bottom of the ice sheet. It should be noted that the air temperature T_a was not taken to be equal to the snow surface temperature T_s.

The ice growth rate was calculated by assuming steady state conditions and neglecting heat transfer between water and ice, as:

$$\frac{dh_i}{dt} = \frac{1}{\rho\lambda} \frac{(T_m - T_a)}{\frac{h_s}{k_s} + \frac{h_i}{k_i} + \frac{1}{H_a}} \qquad [4.1]$$

where ρ_i is the ice density (917 kg/m^3); λ is the latent heat of fusion of ice (3.34x10^5 J/kg); k_i and k_s are thermal conductivity of ice (2.24 W/m^2 °K) and snow respectively; h_i and h_s are the thickness of the ice and snow cover respectively; T_m is the water temperature (assumed to be 0°C); T_a is the air temperature some distance above the snow surface; and H_a is the heat transfer coefficient between snow surface and air. It is of interest to note that for no snow cover on ice, and equal air and ice surface temperature, Equation 4.1 reduces to Stefan's formula (Section 3).

A snow cover on an ice surface acts as an insulating blanket as its thermal conductivity is an order of magnitude lower than that of ice; and this effect is captured in the model. The effect of slush was also included (described subsequently). Should the weight of the snow on the ice be sufficient to cause submergence, then flooding of the snow cover was assumed to occur and slush was formed. No further "bottom ice growth" was allowed to occur until the slush refroze.

Mellor, 1977 related the conductivity of the snow layer to the density of the snow cover, ρ_s. For a range of snow density between 180 and 300 kg/m^3, the relation $k_s = 3.2\text{x}10^{-6}\rho_s^2$ represented the average of the data collected by various researchers, and was used in the model.

The heat transfer coefficient from the snow surface to the air, H_a, can be determined by calculating the heat flux, q_a, using detailed energy budget calculations. Alternatively, this parameter has been found to be related to the wind speed, varying from 10 W/m^2 °K for calm conditions to 25 W/m^2 °K for days with a wind speed of 4 m/s (Ashton, 1986). A sensitivity study suggested that the effect of H_a decreased with increasing the snow cover thickness. To keep their analysis simple, Singh and Comfort, 1998 used a constant value of 25 W/m^2 °K.

"Surface Ice Growth"

Equation 4.1 does not include ice "surface growth" because this involves additional processes. The total ice thickness at any given time is the sum of the "bottom" and the "surface" growth. Ice surface growth results from the freezing of slush formed on the ice surface, as was observed many times during the field observations. This resulted from various mechanisms. Rainfalls added water to the ice surface as well as melting the snow that was already there, and this water and slush subsequently froze. Water reached the ice surface through cracks in the ice sheet which also melted some of the snow that subsequently froze. Other times, rainfalls washed out the snow cover completely especially during a period of warming temperatures.

For deep snow cover, the weight of the snow depressed the ice surface below water level, causing water to flood onto the ice surface through cracks in the ice surface. Not all of the water froze, leaving layers of water above the initial ice surface. This led to a situation where layers of snow, ice, and water were present above the ice sheet that was originally present.

The presence of slush altered the heat budget completely, and the ice surface temperature of ice was brought to about 0°C by this process (as was confirmed by the field measurements). It was found that no "bottom ice growth" could occur until the slush was refrozen. Sometimes the slush never froze, especially for a thick snow cover with the result that the ice growth was terminated for the winter.

Ice surface growth was modeled by noting that the slush re-freezing mechanism is similar to that in Equation 4.1 if slush is considered to be like water near the freezing point. If subzero air temperatures persist, the slush will freeze to form snow ice in the model. The freezing of slush in the model strongly depends on the thickness of the snow cover over the slush.

4.2 Snow Cover Thickness

It is well known that predicting the snow cover thickness even at ground sites is a complex process because it depends on many factors (snowfalls and rainfalls, air temperature, wind speed and direction, local topography, solar radiation, etc.). The problem is further complicated for ice on reservoirs because snow does not begin to accumulate on the reservoir until freeze-up is complete. Also, the weight of the accumulated snow on the ice sheet may submerge it below water level, causing flooding and the formation of slush. The snow cover thickness h_s that would cause flooding can be predicted by balancing the weight of the snow and ice as

$$h_s = (\rho_w/\rho_s)(1-\rho_i/\rho_w)h_i \qquad [4.2]$$

where ρ_i, ρ_s and ρ_w are the densities of ice, snow cover and water, and h_i is the thickness of the ice sheet. Based on the above equation, a snow cover with a density of 200 kg/m^3 and a thickness equal to half the thickness of the ice sheet would be flooded.

Furthermore, once the ice surface is flooded, water will rise into the snow cover by capillary action. The height of this rise depends on the density and the grain size of the snow. Ager, 1962 observed this rise to be between 38 mm and 86 mm for various densities of snow.

All of these factors caused the snow cover on the reservoirs to always be significantly less than that at nearby ground stations during the field projects that were conducted. Singh and Comfort, 1998, recognized that a detailed analysis which accounted for all of these factors and processes would be very complex and uncertain. Furthermore, data to define the required inputs are not available on a long-term systematic basis.

Consequently, they used a simpler empirical approach, based on the snow cover accumulations measured by Environment Canada (EC) at nearby ground stations. It was presumed that these data would reflect all local conditions relevant to reservoir of interest except for: (a) delays in the accumulation of snow due to freeze-up of the reservoir; and (b) loss of snow cover due to

submergence of the ice surface. The snow accumulations measured by EC were "corrected" based on: (a) the reservoir's freeze-up date; (b) the submergence of the snow cover calculated using equation 4.2; and: (c) the expected capillary rise, which was set at 5 cm for the analyses.

4.3 Heat Flow and Ice Temperature

Singh and Comfort, 1998's model was aimed at analysing events that occur on time scales of 1 day or more, because the thermal load events of interest occurred over time periods of more than 1 day, and ususally several days. Consequently, they did not carry out transient analyses; but rather they ran their model in time steps of 1 day, using the mean daily air temeoperaure as an input.

A detailed energy balance would need to account for many terms including energy flux in melting/freezing of ice, convective heat transfer, the net long-wave radiation, the net short-wave radiation and the advected heat transfer to ice by precipitation. However, it is not possible to conduct long-term heat budget analyses as the only long-term historical data are the air temperature, the snowfalls, the rainfalls, and the snow accumulation on the ground.

Due to this limitation, the analyses were performed using a simplified procedure based on a "bulk" heat transfer coefficient H_a (also used in Equation 4.1) between the ice/snow surface and the air. The "bulk" heat transfer coefficient accounts for the boundary layer between ice surface (or snow, if present) and air (Figure 4.1). It was assumed that the heat input to the ice due to precipitation and short-wave radiation was negligible. Heat input from long-wave radiation and convective heat transfer were included in this treatment.

Singh and Comfort, 1998 assumed that ice growth is slow; that the temperature profile in the ice and snow cover is linear; and that the heat flux from water to the ice cover is negligible compared to the heat flux from the ice cover to the snow cover, and from the snow cover to the air. For a steady-state condition, the ice surface temperature, T_i can be determined as:

$$T_i = \frac{\left(h_i / k_i\right) T_a}{\frac{h_s}{k_s} + \frac{h_i}{k_i} + \frac{1}{H_a}} \qquad [4.3]$$

Bergdahl (1978) suggested that a formulation based on a bulk heat transfer coefficient would overestimate the ice surface temperature, and would result in a smaller thermal ice thrust. This is primarily because the short-wave radiation was neglected. This assumption is critical when a large portion of incident solar radiation is absorbed onto the surface. However, when a snow cover is present (which is often the case), about 90% of the incident radiation is reflected. In this case, the error introduced by neglecting short-wave radiation is expected to be minimal.

The heat transfer coefficient in Equation 4.3 could be related approximately to the wind speed, varying from 10 W/m^2 °K for calm conditions to 25 W/m^2 °K for a windy day (Ashton, 1986). To keep the analysis simple, Singh and Comfort, 1998 used a constant value of 25 W/m^2 °K for the heat transfer coefficient. This is a conservative assumption, as it will probably lead to a slight overestimation of the heat flux.

Equation 4.3 is not applicable when the ice sheet is flooded. In this period, the ice sheet is near its melting temperature, and it is not affected by air temperature changes. However, until the slush is frozen, no thermal ice thrust can be developed. Once the ice surface temperature is estimated, the ice temperature profile is calculated, assuming a linear ice temperature profile.

5. A Sample Case for Analysis

5.1 Location and General Ice Cover Regime

Ice thicknesses measured in Lake St Francis were used as a sample case for comparing the results of various ice growth predictors. Lake St Francis is a large lake in the St. Lawrence River upstream of Valleyfield and the Beauharnois Canal (Figure 5.1); and as a result, the currents in it are expected to be low. Ice thicknesses were monitored in the past by Environment Canada at three locations in Lake St Francis (Figure 5.1). The data set covers the period from the 1970-71 to the 1999-2000 winters. A smooth ice cover regularly forms over all of Lake St. Francis (Figure 5.1); and it persists until late-spring.

Location Map

March 18, 2008

March 28, 2008

Figure 5.1 Location Map and Ice Cover Conditions

The ice growth pattern has varied considerably over the winters. Figure 5.2 shows a case where the ice thickness increased steadily over the winter (of 1970-71), reaching a peak in late winter. The ice thickness increased steadily in response to the accumulated Freezing Degree Days (FDDs), at nearby Pierre Elliott Trudeau airport in Montreal. The 1970-71 winter produced the largest measured annual maximum ice thickness.

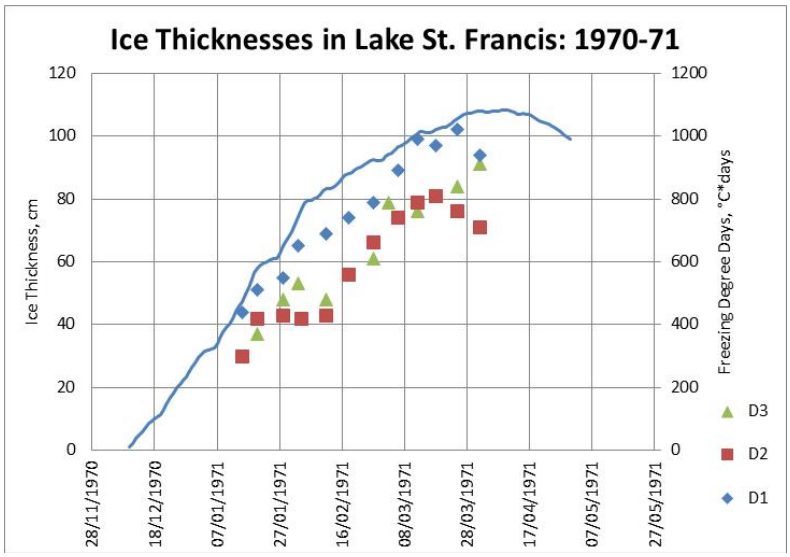

Figure 5.2 Ice Growth Pattern for the 1970-71 Winter

Figure 5.3 shows an example (i.e., the 1984-85 winter) where the peak ice thickness occurred in mid-winter despite the fact that the FDDs continued to increase over the remainder of the winter; while the measured ice thicknesses steadily decreased. It is clear that for this winter, the FDDs would be a poor index for predicting the ice growth pattern.

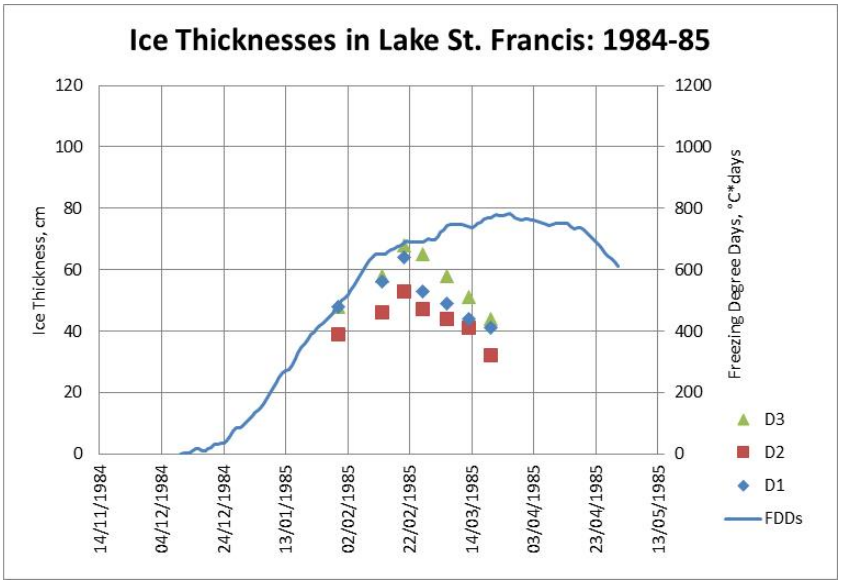

Figure 5.3 Ice Growth Pattern for the 1984-85 Winter

5.2 The Annual Maximum Ice Thickness

The data set was reviewed to determine the maximum ice thickness for each winter. In an effort to ensure that the annual maximum ice thickness was captured in the data, the data set was

limited to winters in which 5 or more ice thickness measurements were made over the course of the winter. This produced a dataset of 12-14 observations (Table 5.1).

Table 5.1 Annual Maximum Ice Thicknesses

	Measured Annual Maximum Ice Thicknesses					100 Yr
	Average	Maximum	Minimum	St. Dev.	# of Obs.	Ice Thickness
Station D1	0.61	1.02	0.36	0.17	14	1.00
Station D2	0.53	0.81	0.37	0.13	12	0.87
Station D3	0.61	0.94	0.41	0.15	13	1.10
D1,D2,D3 Combined	0.63	1.02	0.37	0.16	14	1.05

It can be argued that the ice thickness data form the best basis for extrapolations to longer return periods. Unfortunately, for this case (and for most cases), the data record is short. Also, it is evident that the 1970-71 winter was by far, the most severe one in the period of record, as the peak ice thickness reached during it was much larger than for the other winters (Figure 5.4). This introduces uncertainties as the 1970-71 winter appears to be an outlier; and thus, it is difficult to assess its actual return period based solely on the empirical data.

Another concern with an extreme value method based on ice thickness data is that it is a purely statistical approach. As the return period is increased, the distributions will predict increasing values of the ice thickness regardless of the prevailing environmental conditions, which includes the available freezing degree-days and snow cover. It is possible that the prevailing environmental conditions would prevent the larger ice thickness from being reached (e.g., if insufficient FDDs were available). Thus, this method is expected to produce an upper bound estimate of the annual maximum 100-year ice thickness.

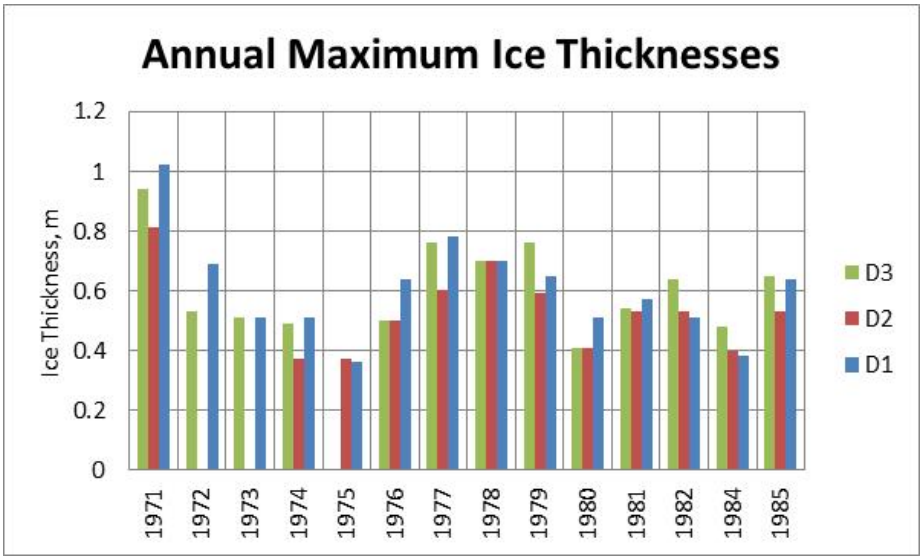

Figure 5.4 Measured Annual Maximum Ice Thicknesses

The annual maximum ice thicknesses were analyzed to determine their distribution. The 1970-71 winter was included in the dataset used for these analyses. The 100-year ice thickness varied from 0.87m to 1.10m depending on the measurement location (Table 5.1 and Figure 5.5).

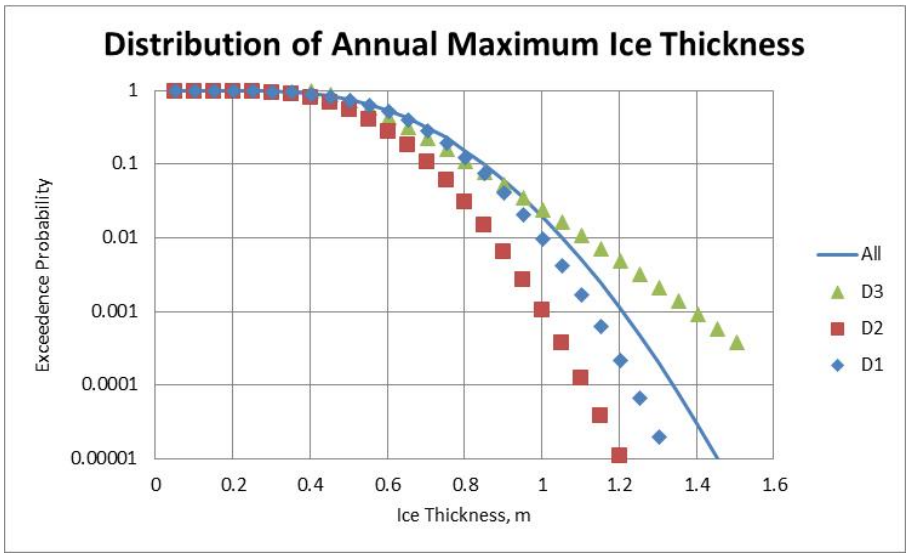

Figure 5.5 Distribution of Annual Maximum Ice Thicknesses

5.3 Freezing Degree Days

The closest source of weather data for Lake St. Francis is Pierre Elliot Trudeau airport in Montreal. Air temperature data were analyzed to determine the FDDs from 1969-70 to 2006-07. The peak FDDs per winter have averaged 821 °C*days ranging from 359 to 1118 °C* days. The best-fit distribution (Figure 5.6) showed that the 100-year FDDs was 1145 °C*days.

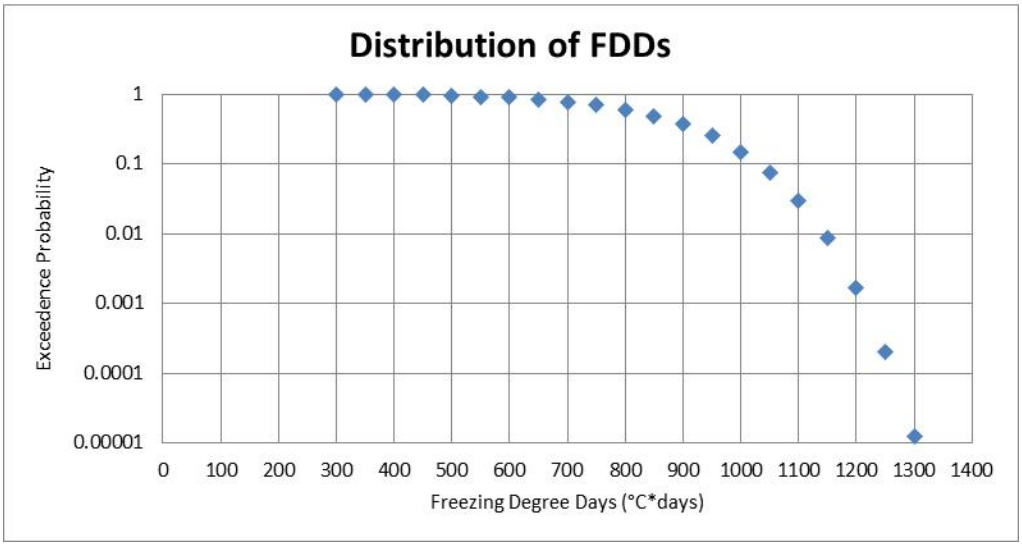

Figure 5.6 Distribution of Peak FDDs per Winter

6. Predicted Ice Thicknesses

6.1 Using the Stefan Equation Without Ice Thickness Data for Calibration

This represents the most basic case in that the engineer would be confronted with the problem of predicting the ice thickness with minimal data. It would be reasonable to presume that Lake St. Francis is an "average lake with snow", in which case, the Stefan equation coefficient, "α", is expected to range from 1.7 to 2.4 (Table 3.1). Using an average value of 2 for "α", and a value of 1145 °C*days for the 100-year FDDs, one obtains a value of 0.68m for the 100-year ice thickness in Lake St Francis. This is much less than the results from the measured ice thickness data which indicated a range of values from 0.87m to 1.1m for the 100-year ice thickness.

6.2 Using the Stefan Equation With Ice Thickness Data for Calibration

This was done by using the measured ice thickness data, in combination with knowledge of the FDDs at the time, to calculate the value of "α" for each measurement. This allowed a dataset of 436 values to be established for "α". The average value for "α" was 1.70 with a range from 0.11 to 3.14. Figure 6.1 shows the best-fit distribution that was determined for "α".

This shows that "α" varied substantially; and it highlights the uncertainties resulting from using a single value of "α" to predict the ice thickness using the Stefan equation. Some of the "α" values seemed unrealistically low, and these were investigated. There were 7 cases where "α" was less than 0.5. They all occurred for thin ice (14 cm or less) in late season; and perhaps, these data points were affected by melting. For a more detailed analysis, this issue should be investigated. This was not done here as judgment would be involved. Also, only sample calculations are being performed and the upper-range ice thicknesses would probably not be substantially affected by this issue. Nevertheless, this highlights another uncertainty associated with the analyses.

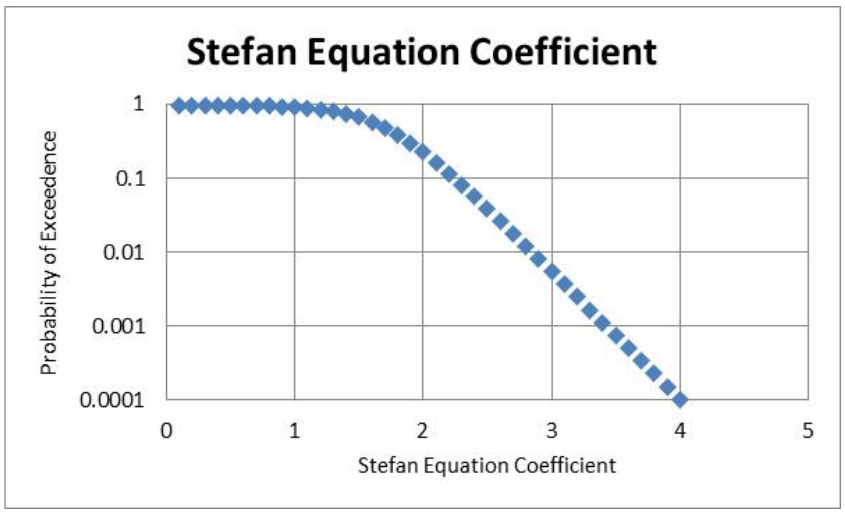

Figure 6.1 Distribution for the Stefan Equation Coefficient

Combined probabilistic analyses were done to predict the 100-year ice load by taking account of the variability in both "α" and the FDDs, by presuming that these two inputs to the Stefan equation are equally uncertain. The ice thickness with a 100-year return period was calculated for various combinations of "α" and FDDs, with each one representing an annual probability of exceedence of 0.01. The 100-year ice thicknesses ranged from 0.73 to 0.78 m (Table 6.1).

Table 6.1 Using the Stefan Equation With Ice Thickness Data For Calibration

FDDs		Stefan Coefficient, "α"		Combined	100-year
Value	Exc. Prob.	Value	Exc. Prob.	Probability	Ice Thickness, m
845	0.50	2.68	0.02	0.01	0.78
950	0.25	2.5	0.04	0.01	0.77
990	0.167	2.4	0.06	0.01	0.76
1010	0.125	2.31	0.08	0.01	0.73

6.3 Results from Singh and Comfort, 1998's Detailed 1-D Model

This model was run for weather data collected at Pierre Elliot Trudeau airport in Montreal, which is within about 30 km of Lake St. Francis. The model was run for the winters from 1969-70 to 2006-07. The annual maximum ice thickness ranged from 0.69m to 1.08m, with an average of 0.90m. The best-fit distribution indicated a value of 1.12m for the 100-year ice thickness (Figure 6.2). This is in reasonable agreement with the results from the extreme value analyses that were done using the measured ice thickness data.

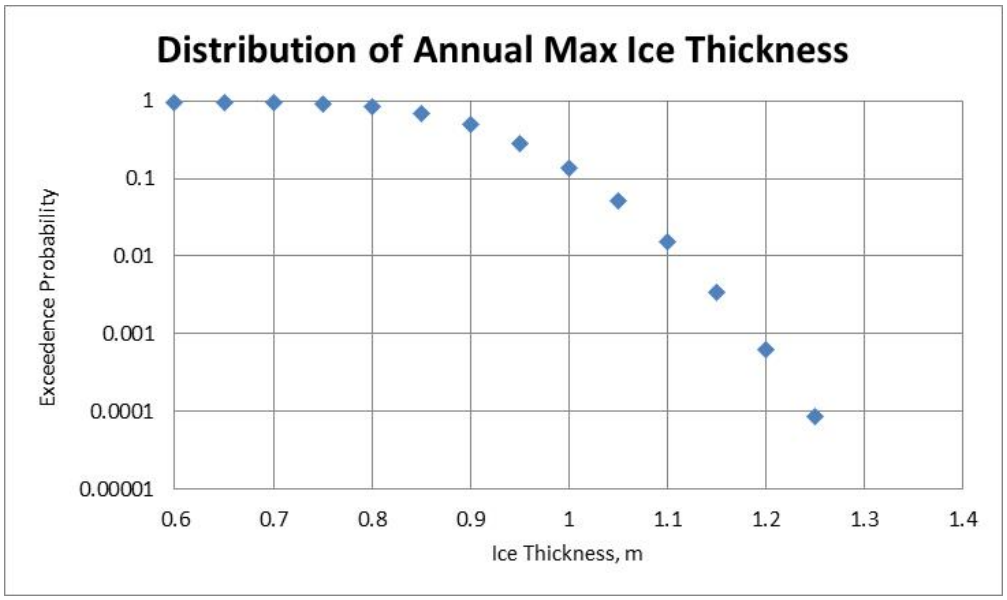

Figure 6.2 Annual Maximum Ice Thickness From the Singh and Comfort, 1998 Model

7. Conclusions

Various methods have been explored for predicting the ice thickness resulting from static ice formation. Each one has its strengths and limitations.

For the case considered here, the simplified methods underestimated the ice thickness obtained using extreme value analyses done with measured ice thickness data. This believed to be due, in large part, to the fact that the simplified models don't account for ice surface growth. This is a serious limitation in some cases.

The sample calculations have shown that simplified methods may be either non-conservative or conservative, depending on the application. For example, conservative results would be obtained by underestimating the ice thickness for bearing capacity analyses. On the other hand, under-estimating the ice thickness would lead to non-conservative results for ice load evaluations.

These results should be extended to a wider range of cases before firm conclusions are drawn.

However, as an overall cautionary comment, the engineer must be aware of these issues and uncertainties in establishing design ice thicknesses.

References

Ager, B., 1962, Studies on the Density of Naturally and Artificially Formed Freshwater Ice, Journal of Glaciology, Vol. 4, no. 32, pp. 207-214.

Ashton, G., 1986, River and Lake Ice Engineering, Water Resources Publications, Littleton, Col.

Bergdahl, L., 1978, Department of Hydraulics, Thermal Ice Pressure in Lake Ice Covers, Chalmers University of Technology, Sweden, Report Series A:2.

Comfort, G., Gong, Y., Singh, S., and Abdelnour, R., 2003a, Static Ice Loads on Dams, CSCE Special Journal on River Ice, Canadian Journal of Civil Engineering, 30:42-68(2003).

Comfort, G., Gong, Y., and Liddiard, A., 2003b, Static Ice Loads on Dams, International Conference On Large Dams (ICOLD) Montreal, Quebec.

Gilbert, R., and Glew, J., 1986, A Wind-Driven Ice Push Event in Eastern Lake Ontario, Journal of Great Lakes Research 12(4): 326-331.

Morse, B., Ringo, B, Stander, E., Robert, J., Messier, D., and Quach, T., 2009, Growth and Decay of Estuary Ice Cover, Journal of Cold Regions Engineering, September, 2006.

Singh, S, and Comfort, G., 1998, Expected Thermal Loads in Reservoirs, proc. IAHR Ice Symposium, Potsdam, NY.

USACE, 2002, Engineering and Design Manual: Ice Engineering, Engineer Manual EM-1110-2-1612, United States Army Corps of Engineers.